View Online / Journal Homepage / Table of Contents for this issue
Dynamic Article Links

Green Chemistry

Cite this: *Green Chem.*, 2011, **13**, 702

www.rsc.org/greenchem

PAPER

Highly active and green aminopropyl-immobilized phosphotungstic acid on mesocellular silica foam for the *O*-heterocyclization of cycloocta-1,5-diene with aqueous H_2O_2†

Ruihua Gao,[a,b] Quanjing Zhu,[a] Wei-Lin Dai*[a] and Kangnian Fan[a]

Received 15th October 2010, Accepted 6th December 2010
DOI: 10.1039/c0gc00691b

The heteropoly phosphotungstic acid, $H_3PW_{12}O_{40}$ (HPW), was successfully immobilized on the surface of MCF, SBA-15 and MCM-41 by means of chemical bonding to aminosilane groups. The as-obtained materials were characterized by N_2 sorption, TEM, XRD, FT-IR, ^{13}C-, ^{29}Si-, ^{31}P-MAS NMR and XPS. Characterization results suggest that the surface area decreased after grafting amino groups to silica. The as-prepared HPW-NH_2-MCF is highly efficient in the *O*-heterocyclization of cycloocta-1,5-diene (COD) to 2,6-dihydroxy-9-oxabicyclo[3.3.1] nonane (**1**) and 2-hydroxy-9-oxabicyclo [3.3.1] nonane-6-one (**2**) with a COD conversion of 100% and (**1** + **2**) selectivity up to 98%. It is worth mentioning that this material could be reused six times without any significant loss of activity and selectivity. The good stability can be attributed to the strong interaction between the amino groups on the surface of MCF and HPW anions.

1. Introduction

γ-Butyrolactone structure is an important intermediate in organic synthesis since lots of compounds containing this functional group show interesting biological activity.[1–3] For instance, 5-hydroxy-γ-decalactone is a potent cytotoxic agent on different tumor cell lines.[4]

It is commonly accepted that 9-oxabicyclo[3.3.1]nonane-2,6-dioles (**1**) and 2-hydroxy-9-oxabicyclo[3.3.1]nonane-6-one (**2**) are the major starting materials for the synthesis of γ-butyrolactones. Therefore, it is of great significance to develop efficient and accessible approaches to afford these products (**1** and **2**). Traditional routes for **1** and **2** employ peroxo-acid or permanganate as oxidants. Behr *et al.* obtained 23.3% yield of **1** by using peracetic acid as the oxidant and cycloocta-1,5-diene (COD) as the raw material.[5] If peracetic acid was replaced by permanganate, much lower conversion of COD was observed. Moreover, **1** yield can reach 70% if performic acid was used as oxidant, as reported by Hegemann *et al.*[6] However, the use of performic acid, as well as peracetic acid and permanganate, is unsafe, corrosive and costly, and will produce huge amounts of waste. Therefore, it is highly desirable to improve the conventional process by safer and cleaner oxidizing agents, and easily separable catalysts with more activity and selectivity. One effective way to produce these two compounds (**1** + **2**) is the selective oxidation of COD with environmentally benign aqueous H_2O_2 as the oxidant. Since no noxious substances are needed and no toxic waste would be generated in the reaction, hence, it can be called as a green process.

In our previous work, tungstic acid was reported as an efficient homogeneous catalyst for the target reaction.[7] However, the difficulties of separating and recovering the catalysts from the product mixture during the homogeneous process made them impractical for a large-scale process. One of the most promising approaches is to design a heterogeneous WO_3-containing heterogeneous catalyst. In our previous work, we reported the synthesis of a novel tungsten trioxide containing silica with ultra large mesopores and its catalytic application in the *O*-heterocyclization of COD.[8] Although WO_3-containing mesocellular silica foam (MCF) catalysts have been found to show high activity in this reaction, there is detectable leaching of tungsten species from 10% WO_3-MCF according to ICP-AES analysis. It is known that the leaching of tungsten species is inevitable in most reactions with H_2O_2. Hence, there is a strong driving force to find a more stable catalyst without any leaching of tungsten species, so that no heavy metal containing waste water is generated and the catalyst can be reused many times.

Heteropolyacids (HPAs) are early transition metal oxygen anion clusters.[9] Among the various HPA structural classes, Keggin-type[10] HPAs have been widely used as homogeneous

---

[a] *Shanghai Key Laboratory of Molecular Catalysis and Innovative Materials, Department of Chemistry, Fudan University, Shanghai, 200433, P.R. China. E-mail: wldai@fudan.edu.cn; Fax: +86-21-55665701*
[b] *Research Center of Nano Science and Technology, Shanghai University, Shanghai, 200234, P.R. China*

† Electronic supplementary information (ESI) available: See DOI: 10.1039/c0gc00691b

and heterogeneous catalysts for acid–base and oxidation reactions.[11–15] The Keggin-type HPA has a soccer ball-shape with a molecular size of *ca.* 1 nm.[16] One of the disadvantages of HPA catalysts is that their surface area is very low (<10 m^2 g^{-1}). To overcome this problem, HPA catalysts have been supported on inorganic porous materials including mesoporous molecular sieve (MCM-41,[17] SBA-15[18]), carbon gel,[19] and mesoporous γ-alumina[20] by an impregnation method. However, there is obviously detectable leaching of active species from these catalysts. In recent years, another promising approach to obtain HPA catalyst with high surface area is to take advantage of the overall negative charge of the heteropolyanions. By using this method, HPA was immobilized on the polymer materials such as poly-4-vinylpyridine,[21] polyaniline,[22] and polystyrene[23] to obtain molecularly dispersed HPA catalysts. However, such procedure has been restricted when inorganic supporting materials are utilized due to the difficulty in forming a positive charge on inorganic supporting materials. Recently, a successful example for the immobilization of HPA catalyst on an inorganic support has been found.[24] It was reported that $H_3PMo_{12}O_{40}$ was chemically immobilized on a kind of porous carbon by forming a positive charge on the support *via* surface modification.[24] However, no attempt has been made to immobilize $H_3PW_{12}O_{40}$ on the aminopropyl-functionalized MCFs.

MCFs with well-defined ultra large mesopores and hydrothermally robust frameworks are firstly described through an oil-in-water microemulsion method by Winkel *et al.*[25] The MCF materials gain many benefits from their facilitated synthesis method, such as well defined pore and wall structure, thick walls, and high hydrothermal stability, which give MCFs unique advantages as catalyst supports. The HPW/MCF catalysts were firstly synthesized by traditional impregnated method in the present study. Although good performance of the HPW/MCF catalyst was obtained in the title reaction, the obvious leaching of the active tungsten species was also observed. In contrast, the novel HPW-NH_2-MCF catalyst shows better stability and reusability.

In this work, MCF-type silica was prepared *via* oil-in-water microemulsion method. The as-obtained MCF silica was then modified by APTES to provide sites for the immobilization of HPW. By taking advantage of the overall negative charge of $[PW_{12}O_{40}]^{3-}$, the HPW catalyst was chemically immobilized on the surface of modified MCF (NH_2-MCF) silica as a charge matching component. The characteristics of HPW catalyst immobilized on the NH_2-MCF silica were extensively characterized in terms of various physicochemical techniques.

2. Experimental

2.1 Catalyst preparation

The MCF materials were prepared following a procedure similar to that reported by Winkel *et al.*[25] Fig. 1 shows the schematic procedures for the surface modification of MCF silica and the subsequent immobilization of HPW on the surface of modified MCF (NH_2-MCF) silica. The surface modification of the MCF silica was achieved by reacting the silanol group of the MCF silica with APTES (Aldrich) under a nitrogen atmosphere. 2.3 mmol of APTES was slowly added to a dry toluene solution containing 1 g of MCF silica, SBA-15[26,27] and MCM-41[28] with constant stirring at room temperature. These solid products were filtered and dried at 100 °C for 2 h to yield the NH_2-MCF, NH_2-SBA-15 and NH_2- MCM-41 silica, respectively.

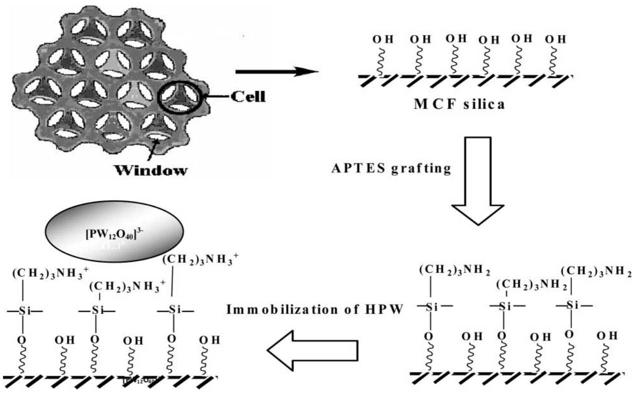

Fig. 1 Schematic procedure for the surface modification of MCF silica and the subsequent immobilization of HPW on the surface modified MCF (NH_2-MCF) silica.

The immobilization of HPW on the NH_2-MCF silica support was carried out as follows (shown in Fig. 1). 1 g of NH_2-MCF silica, NH_2-SBA-15 or NH_2-MCM-41 was added to an aqueous solution containing HPW (0.36 g) with vigorous stirring at 60 °C, and the resulting solution was maintained at 60 °C for 24 h. These solid products were filtered, washed with distilled water three times and then dried overnight at 80 °C to yield the 16%HPW-NH_2-MCF, HPW-NH_2-SBA-15 and HPW-NH_2-MCM-41 silica samples. The 8%, 24% and 30% HPW-NH_2-MCF were synthesized using the same method, only with different volumes of HPW aqueous solution.

The impregnation method derived HPW/MCF-1 catalyst was synthesized as follows. 0.36 g of HPW was dissolved in deionized water. Then 1 g of MCF was added into the stirred solution at 60 °C. After being stirred for 8 h, the solid was filtered, washed with distilled water, and dried at 80 °C (denoted as 16%HPW/MCF-1). Inductively coupled argon plasma (ICP) analysis indicated that the tungsten weight content of the 16%HPW/MCF-1 was 0.04%, suggesting that more than 99% loosely bonded HPW species were readily removed after washing with distilled water.

The impregnation method derived HPW/MCF-2 catalyst was synthesized as follows. 0.36 g of HPW was dissolved in distilled water. Then 1 g of MCF was added into the stirred solution at 60 °C. After being stirred for 8 h, the excessive water was completely evaporated at the same temperature under depressed pressure and the catalyst was finally obtained after the solid material was dried at 80 °C in air for 3 h (denoted as 16%HPW/MCF-2).

2.2 Characterizations

The specific surface area, pore volumes and the average pore size of the samples were measured and calculated according to the BET method on Micromeritics TriStar 3000 equipment with liquid nitrogen at −196 °C. Transmission electron micrographs (TEM) were obtained on a JOEL JEM 2010 scan-transmission electron microscope. The wide-angle X-ray powder diffraction (WAXS) patterns were recorded on a Bruker D8 advance diffractometer with Cu-Kα radiation, operated at 40 mA and 40 kV.

The FT-IR measurements were carried out with a Nicolet Model 205 spectrometer, using KBr pellet technique. The ^{29}Si, ^{13}C and ^{31}P CP-MAS NMR spectra of the solid catalysts were collected in a Brucker DXR 400 spectrometer.

The XPS spectra were recorded on a Perkin-Elmer PHI 5000C ESCA system equipped with a dual X-ray source, using the Mg-Kα (1253.6 eV) anode and a hemispherical energy analyzer. The background pressure during data acquisition was kept below 10^{-6} Pa. Measurements were performed at pass energy of 93.90 eV to ensure sufficient sensitivity for the acquisition scan, and pass energy of 23.50 eV was used for the scanning of the narrow spectra of Si 2p, W 4f, O 1s, N 1s and C 1s to ensure sufficient resolution. All binding energies were calibrated using contaminant carbon (C 1s = 284.6 eV) as a reference. The tungsten content was determined by ICP method (IRIS Intrepid, Thermo Elemental Company) after solubilization of the samples in HF : HCl solutions.

2.3 Catalytic reaction: COD oxidation

The activity test was performed at 60 °C for 20 h with magnetic stirring in a closed 25 mL regular glass reactor using 50% aqueous H_2O_2 as oxygen-donor and *t*-BuOH as the solvent. In a typical experiment, 1.06 mL of COD, 10 mL of *t*-BuOH and 0.2 g of the HPW-NH_2-MCF material (16%) were introduced into the regular glass reactor at 60 °C with vigorous stirring. The reaction was started by adding 1.4 mL of 50 wt% aqueous H_2O_2 into the mixture and was kept for additional 20 h. The quantitative analysis of the reaction products were performed by using GC method and the identification of different products in the reaction mixture was determined by means of GC-MS on HP 6890GC/5973 MS.

3. Results and discussion

3.1 Characterization of the HPW-NH_2-MCF catalysts

N_2 adsorption isotherms of different HPW-NH_2-MCF samples are recorded. The irreversible-type IV adsorption isotherms with H1 hysteresis loop defined by IUPAC are observed, that is a typical feature of mesoporous materials (not shown here). The textural parameters of catalysts with different HPW loadings were listed in Table 1. The surface area of the NH_2-MCF silica was decreased with incorporation of APTES. The HPW-NH_2-MCF silica showed a much lower surface area than the corresponding NH_2-MCF silica, due to the loading of the HPW species. The surface area of the HPW-NH_2-MCF silica dropped along with the increasing amount of HPW. We can also find the pore size order of these samples: 16% HPW-NH_2-MCF > 16% HPW-NH_2-SBA-15 > 16% HPW-NH_2-MCM-41, which is in the same trend with their parent materials.

ICP results of the catalysts with different HPW loadings are shown in Table 2. The concentration of amino group was 2.2 mmol g^{-1} as determined by TG method. The tungsten content of the HPW-NH_2-MCF catalysts increases with the increasing amount of HPW used. However, the tungsten content of the 30%HPW-NH_2-MCF is similar to that of the 24% one, indicating that the modified silica has a maximal saturated value for the percentage of HPW stably incorporated on the surface. In addition, we also attempted to support HPW on pure MCF silica. In this case, however, the HPW species were almost completely dissolved out from 16%HPW/MCF-1 during the washing step (see Table 2). In other words, HPW species could not be successfully immobilized on the surface of unmodified MCF silica, due to the absence of anchoring sites for the HPW species. The above results imply that the surface modification of MCF silica to provide anchoring sites for HPW species is essential for the successful immobilization of HPW species on MCF silica.

TEM images (Fig. 2) of 16%HPW-NH_2-MCF materials revealed a disordered array of silica struts composed of uniform-sized spherical cells interconnected by windows with a narrow size distribution, which is the characteristic structural feature

Table 1 Physico-chemical parameters of various samples

Material	S_{BET} (m^2 g^{-1})	Vp (cm^3 g^{-1})	Dc (nm)[a]	Dw (nm)[b]
MCF	592	1.37	18.9	5.1
NH_2-MCF	303	0.88	15.8	4.5
8%HPW-NH_2-MCF	263	0.83	12.8	4.0
16%HPW-NH_2-MCF	170	0.55	12.7	4.9
24%HPW-NH_2-MCF	122	0.35	12.1	4.8
30%HPW-NH_2-MCF	122	0.33	11.7	4.5
SBA-15	760	1.37	7.3	—
NH_2-SBA-15	407	0.80	6.9	—
16%HPW-NH_2-SBA-15	284	0.56	6.5	—
MCM-41	926	0.84	3.2	
NH_2-MCM-41	759	0.54	3.0	
16%HPW-NH_2-MCM-41	434	0.21	3.0	—
16%HPW/MCF-1	545	1.0	16.8	4.0
16%HPW/MCF-2	439	0.8	10.5	3.6

[a] Cell diameter. [b] Window diameter, determined according to the BJH method. The 16%HPW/MCF-1 and 16%HPW/MCF-2 was synthesized as described in the experimental section.

Table 2 ICP results of the different catalysts over different HPW loadings[a]

Samples	W (%)	mmol amine/g silica	mmol HPW/ g silica	mol HPW/ mol amine
8% HPW-NH_2-MCF	6.2	2.2	0.028	0.0127
16% HPW-NH_2-MCF	15.6	2.2	0.071	0.0323
24% HPW-NH_2-MCF	23.0	2.2	0.104	0.0473
30% HPW-NH_2-MCF	24.2	2.2	0.109	0.0495
16% HPW/MCF-1	0.04	0	0.0002	—
16% HPW/MCF-2	15.8	0	0.072	—

[a] Determined according to the ICP-AES method.

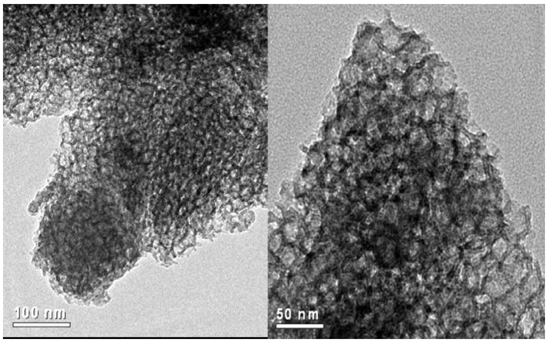

Fig. 2 TEM images of 16%HPW-NH_2-MCF catalyst.

of the MCF materials.[25,29] This result clearly indicates that the samples keep the pore structure of the support very well.

Fig. 3 shows the XRD patterns of pure HPW, NH_2-MCF and HPW-NH_2-MCF samples. The pure HPW catalyst showed the characteristic Keggin XRD pattern of heteropoly acids. On the other hand, NH_2-MCF silica and HPW-NH_2-MCF samples showed no characteristic XRD pattern due to the amorphous nature of MCF silica. It is interesting that 8–24% HPW-NH_2-MCF all showed no characteristic Keggin structure in their XRD patterns, indicating that the HPW species were not in a crystalline state but in a highly dispersed amorphous-like state. This finding demonstrates that the HPW species are finely and molecularly dispersed on the surface of NH_2-MCF *via* chemical interaction. As attempted in this work, it is believed that heteropolyanions were strongly immobilized on NH_2-MCF as charge compensating components. However, 16%HPW/MCF-2 catalyst shows sharp XRD peaks of HPW (see Figure S1 in ESI†), indicating that the keggin-type structure was kept well in the impregnated-method derived catalyst.

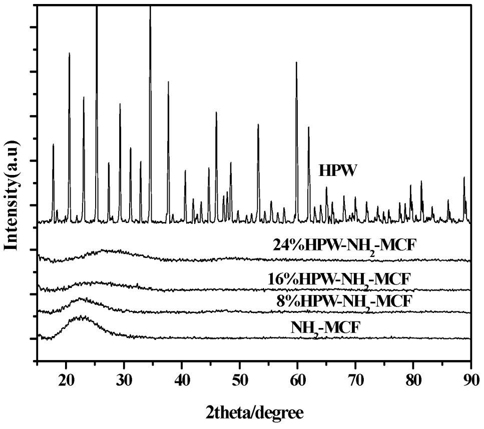

Fig. 3 X-Ray diffraction patterns of HPW-NH_2-MCF catalysts.

^{29}Si MAS NMR spectra (Fig. 4) of the amino group functionalized MCF showed three up-field resonance peaks corresponding to Q^4 (–111 ppm), Q^3 (–101 ppm) and Q^2 (–92 ppm), and two down-field peaks, assigned to T^3 (–67 ppm) and T^2 (–58 ppm), respectively, where $Q^n = Si(OSi)_n(OH)_{4-n}$, $n = 2–4$ and $T^m = RSi(OSi)_m(OH)_{3-m}$, $m = 1–3$. The presence of T peaks confirms the incorporation of the aminosilane moieties as a part of the silica wall structure.[30,31]

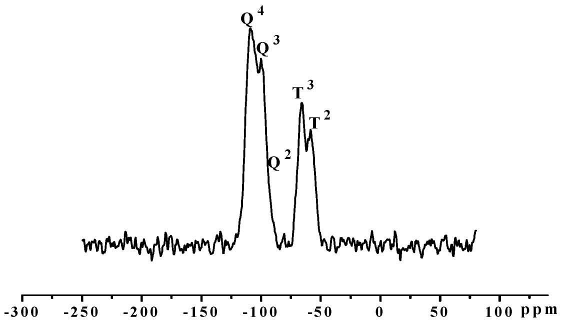

Fig. 4 The ^{29}Si MAS NMR of NH_2-MCF material.

Fig. 5 shows the solid-state ^{13}C CP-MAS NMR spectra of NH_2-MCF silica and 16%HPW-NH_2-MCF, which obviously showed three chemical shifts at δ = 43 (C1), 22 (C2), and 9(C3) ppm, while MCF silica exhibited no resonance peak (not shown here). The three resonance peaks observed in the NH_2-MCF were attributed to different carbon atoms (C1, C2, and C3) in the molecular structure of APTES.[32,33] This finding indicates that aminopropyl functional groups were successfully grafted on the MCF silica.

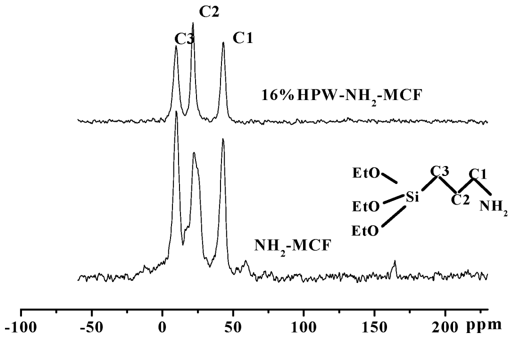

Fig. 5 The ^{13}C MAS NMR of NH_2-MCF and 16%HPW-NH_2-MCF catalyst.

The successful immobilization of the HPW catalyst on the aminopropyl-functionalized MCF silica can also be confirmed by FT-IR analyses as shown in Fig. 6. A band at 1630 cm^{-1} observed in all the samples can be assigned to the –OH vibration of physisorbed H_2O. In the case of NH_2-MCF and HPW-NH_2-MCF, the Si–O–Si band originated from MCF silica were observed at around 1000–1250, 805 and 475 cm^{-1}. A broad band at 2700–3400 cm^{-1} and a weak band at around 1520 cm^{-1} observed in NH_2-MCF and HPW-NH_2-MCF are attributed to the $–NH_3^+$ stretching vibration, indicating the presence of aminopropyl functional group in NH_2-MCF and HPW-NH_2-MCF.[30,34] The primary structure of unsupported HPW can be identified by the four characteristic IR bands appearing at 1076 cm^{-1} (P–O band), 982 cm^{-1} (W–O bands), 882 and 806 cm^{-1} (W–O–W bands). The characteristic IR bands of $[PW_{12}O_{40}]^{3-}$ in the HPW-NH_2-MCF were different from those of the unsupported one. The P–O band in the HPW-NH_2-MCF sample was not clearly identified due to the overlapping by the broad Si–O–Si band. However, W–O and W–O–W bands of $[PW_{12}O_{40}]^{3-}$ in the HPW-NH_2-MCF sample appeared at slightly red-shift positions (944 cm^{-1}) compared to those of the unsupported one, indicating

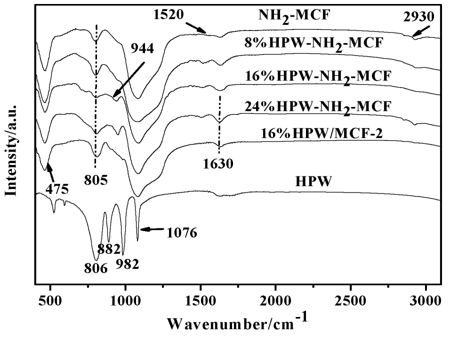

Fig. 6 FT-IR of different HPW-NH_2-MCF catalysts.

the presence of a strong interaction between $[PW_{12}O_{40}]^{3-}$ and NH_2-MCF silica.[24]

^{31}P MAS-NMR is a useful tool in detecting the local environments of HPW, since the chemical shift of the phosphorous atom depends not only on its local environment within the metal cluster but also on factors such as associated water molecules, metal ions, solid supports, and thermal treatments.[35,36] Fig. 7 shows the ^{31}P MAS-NMR spectra of unsupported bulk HPW, HPW-NH_2-MCF, and HPW/MCF. Bulk HPW exhibited a sharp, intense peak at –15.3 ppm, typical of Keggin structures.[35] The sharp peak indicates the presence of P in a highly uniform environment in a hydrated structure of POM. After immobilization, the ^{31}P NMR peaks were found to shift to up-field. The up-field shift reflects the interaction of $[PW_{12}O_{40}]^{3-}$ with the cationic mesoporous silica support. The shift in peak position and decrease in the peak width can also be associated with the loss of water molecules during POM loading.[37] It is interesting to note that the up-field shift was more exaggerated for 8%HPW-NH_2-MCF than that for 24%HPW-NH_2-MCF. This difference in behavior for the two samples can be attributed to a higher HPW loading in the 24%HPW-NH_2-MCF sample, in which excessive HPW particles show some low condensed polymeric HPW species character. Meanwhile, the HPW species of 8%HPW-NH_2-MCF are presented as isolated species. In addition, the peak of 16%HPW/MCF-2 is similar to that of the bulk HPW, indicating that the HPW species of 16%HPW/MCF-2 shows some bulk character of HPW. Thus, the HPW species are not well dispersed on the MCF support. This finding indicates that there is weak interaction of HPW with the mesoporous silica support for the traditional impregnation method.

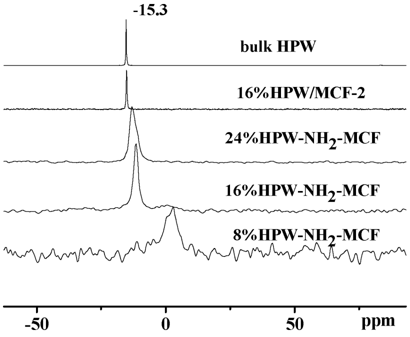

Fig. 7 The ^{31}P MAS-NMR of various samples.

To understand the interaction between the silane moieties and the HPW species, an XPS measurement was performed to compare the N 1s binding energy before and after the adsorption. When compared with the one before HPW adsorption (Fig. 8), the N 1s spectrum showed a high-energy shift from 399.4 to 401.9 eV (~2.5 eV) after the adsorption. This chemical shift has been assigned to an acid–base interaction between the NH_2 groups in the silane moieties and HPW molecules,[38] thus confirming the strong chemical bonding interaction between HPW and the amino groups on the surface of MCF.

3.2 Activity test

According to the GC-MS analysis of the product mixture, as shown in Scheme 1, besides the two main products **1** and **2**, a variety of the byproducts, including **3**, **4** and **5**, are observed, which are all the oxidation derivatives from the epoxide of one C═C bond. It is a surprise to find that there are no cleavage products from one or two C═C bonds, suggesting that only epoxidation of one C═C bond and *O*-heterocyclization of two C═C bonds occurred under the present conditions. Since the two main products **1** and **2** can all be oxidized to the same product – γ-butyrolactones – the total yield of these two products is used to determine the catalytic performance of different catalysts.

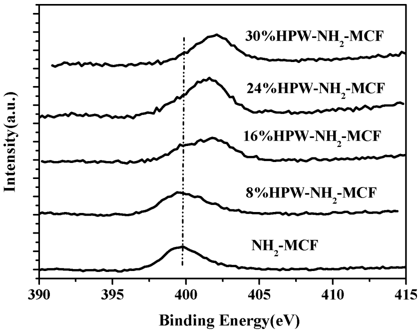

Fig. 8 XPS spectra of the N 1s region for different HPW-NH_2-MCF catalysts.

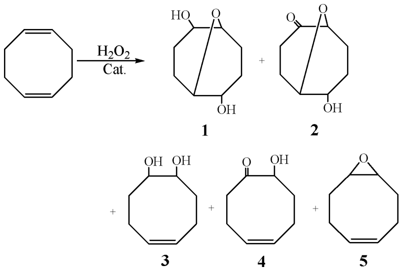

Scheme 1 The products distribution of the oxidation of COD by H_2O_2.

The results of the selective oxidation of COD to **1** and **2** over the HPW-NH_2-MCF catalysts with different HPW loadings and pure HPW are listed in Table 3. The homogeneous HPW show very high catalytic performance for the reaction, however, it is difficult to separate the HPW from the product mixture. For the purpose of comparison, the catalysts used in these experiments contain the same amounts of HPW. It can be seen that the catalytic performance of 16%, 24% and

Table 3 Catalytic performance of the selective oxidation of COD over various catalysts[a]

Catalyst	C_{COD} (%)	S_1 (%)	S_2 (%)	S_{1+2} (%)
HPW-NH_2-MCF (8%)	91.0	31.0	6.9	37.9
HPW-NH_2-MCF (16%)	100	68.8	29.2	98.0
HPW-NH_2-MCF (24%)	100	62.0	37.0	99.0
HPW-NH_2-MCF (30%)	100	45.7	52.7	98.4
HPW/MCF (16%)-1	0.02	2.9	3.7	6.6
HPW/MCF (16%)-2	100	36.4	60.6	97.0
HPW[b]	100	62.1	36.8	98.9

[a] Reaction conditions: reaction temperature 60 °C, H_2O_2 22.5 mmol, cat. 0.2 g, reaction time 12 h, *t*-BuOH 10 mL. [b] HPW = 0.202 g.

Table 4 Reusability of 16%HPW-NH_2-MCF and 16%HPW/MCF-2[a]

Catalyst	Entry	C_{COD} (%)	$C_{H_2O_2}$ (%)	S_1 (%)	S_2 (%)	S_{1+2} (%)
HPW-NH_2-MCF	1	100	98.0	68.8	29.2	98.0
	2	100	97.5	67.6	28.8	96.4
	3	100	94.5	66.5	31.3	97.8
	4	100	97.0	64.4	32.9	97.3
	5	100	96.7	67.2	29.2	96.4
	6	99.0	95.8	67.5	28.9	96.4
HPW/MCF-2	1	100	96.0	36.4	60.6	97.0
	2	99.0	91.5	60.2	32.1	92.3
	3	45.0	21.0	16.4	11.6	28.0

[a] Reaction conditions: reaction temperature 60 °C, H_2O_2 22.5 mmol, cat. 0.2 g, reaction time 12 h, *t*-BuOH 10 mL.

30%HPW-NH_2-MCF are better than that of 8%HPW-NH_2-MCF for this reaction, in terms of the conversion of COD and the selectivity of (**1** + **2**). When tungsten content is higher than 16%, much higher conversion (100%) and excellent selectivity at (~98%) were obtained. The different catalytic performance of these catalysts can be attributed to the different content of active tungsten species. Because the amount of the catalyst is 0.2 g, the total tungsten is different among various catalysts. The tungsten content of the HPW-NH_2-MCF catalysts increases with the increasing amount of HPW used. However, the tungsten content of the 30%HPW-NH_2-MCF is similar to that of the 24% one. The active species of 8%HPW-NH_2-MCF are not enough for the title reaction, and that of the 16% and 24%HPW-NH_2-MCF are enough for the reaction. It should be pointed out that pure MCF is inert to this reaction as confirmed in our previous work. It is also found that the catalytic performance of the fresh 16%HPW/MCF-2 is similar to that of 16%HPW-NH_2-MCF, not only in terms of the conversion of COD, but also in terms of the selectivity to the target products. However, the catalytic performance of 16%HPW/MCF-1 is very poor, similar to that of the blank MCF support. Therefore, it can be speculated that the low tungsten content may be the key factor for the extremely low catalytic activity. From the above characterisations, the HPW species in all the catalysts with different loadings are highly dispersed on the surface of NH_2-MCF. This result suggests that the HPW species incorporated into the uniform framework of mesoporous MCF materials act as the precursor of active centers for the selective *O*-heterocyclization of COD.

The reusability and regeneration of 16%HPW-NH_2-MCF and 16%HPW/MCF-2 are also listed in Table 4. The COD conversion and total selectivity of (**1** + **2**) over the immobilized method derived 16%HPW-NH_2-MCF catalyst decrease slowly and still keep above 99% and 96% after the 6th cycle, while these two values over 16%HPW/MCF-2 catalyst are only 45 and 28% after 3rd cycles of the reaction. This finding clearly indicates that the immobilized method derived 16%HPW-NH_2-MCF catalyst shows much better stability and can be reused for at least 6 times (selectivity of (**1** + **2**) > 96%), while the impregnation-method derived one can only be used once. That is why the HPW materials are very difficult to be applied in commercial plants. To investigate the stability of the active tungsten species in the 16%HPW-NH_2-MCF catalyst, the reaction mixture and the tungsten remaining in the catalyst were also determined by ICP analysis after five reaction cycles. No detectable leaching of W-species or obvious loss of tungsten in the 16%HPW-NH_2-MCF catalyst could be observed, however, the leaching of tungsten species from 16%HPW/MCF-2 is 0.12% in one reaction cycle. Therefore, it can be concluded that the interaction between the active HPW species and the silica-based matrix of MCF by immobilized method is much stronger than that of HPW/MCF-2 prepared by traditional impregnated method. To the best of our knowledge, the as-prepared 16%HPW-NH_2-MCF material in the *O*-heterocyclization of COD is the first example for HPW-based catalysts without any leaching of tungsten species and loss of catalytic activity with H_2O_2 as the oxidant.

The results of COD oxidation over HPW-containing MCF, SBA-15 and MCM-41 are shown in Fig. 9. Comparison of 16%HPW-NH_2-MCF, 16%HPW-NH_2-SBA-15 and 16% HPW-NH_2-MCM-41 reveals that 16%HPW-NH_2-MCF is the most effective one. The results of 16%HPW-NH_2-SBA-15 is similar to that of 16%HPW-NH_2-MCF. The 16%HPW-NH_2-MCM-41 shows the worst catalytic performance. This phenomenon uncovers that the ultra large pores and the unique three dimensional cell-window of MCF are more favorable for the title reaction than the MCM-41 counterpart owning only the small pores and two dimensional pore structures. The good catalytic performance of 16%HPW-NH_2-SBA-15 can also be attributed to its large pores. These results indicate that the pore size may be an important factor on the catalytic performance.

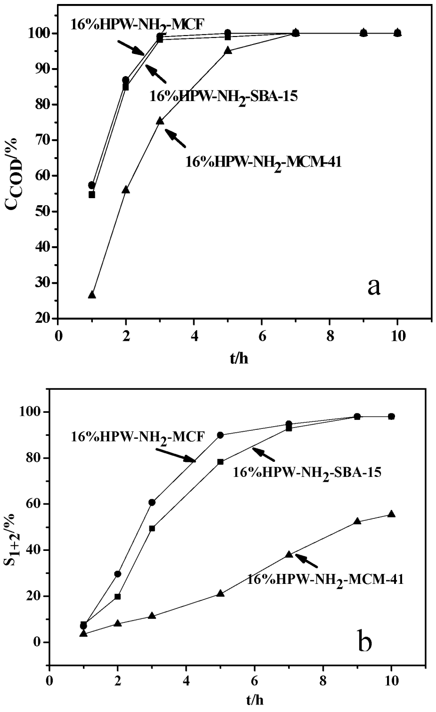

Fig. 9 The conversion of COD (a) and the selectivity to (**1** + **2**) (b) with time over the different catalysts.

In addition, another experiment has been carried out to test whether this novel 16%HPW-NH_2-MCF catalyst is actually a heterogeneous one (Fig. 10). When the reaction over 16%HPW-NH_2-MCF catalyst has been carried out for 1 h, the catalyst is removed through simple filtration and the reaction solution is stirred for another 4 h. No detectable increase of COD conversion in the next 4 h of reaction is observed, indicating that

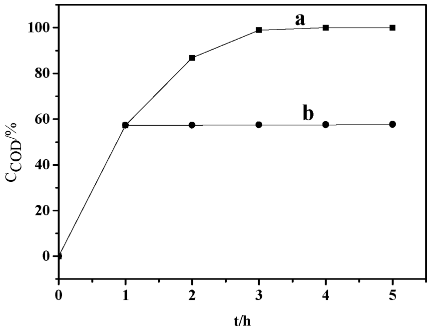

Fig. 10 The conversion of COD with time over the 16%HPW-NH_2-MCF and the filtration (a, with catalyst; b, without catalyst).

the 16%HPW-NH_2-MCF catalyst is actually a heterogeneous one. It is also interesting to find that the addition of new COD to the solution which has been left stirring for normal 12 h after which the heterogeneous catalyst was removed, the conversion of COD for another 12 h was zero. In view of the excellent activity, selectivity and stability of the HPW-NH_2-MCF material in the selective oxidation of COD with aqueous H_2O_2, further studies on the utilization of this material in other organic oxidations including epoxidation and oxidative cleavage of C═C bonds with aqueous H_2O_2 are under way.

4. Conclusion

In summary, the heteropoly phosphotungstic acid, $H_3PW_{12}O_{40}$, has been successfully immobilized on the surface of mesoporous MCF, SBA-15 and MCM-41 by means of chemical bonding to aminosilane groups. Characterization results from N_2 sorption indicate that the surface area decreased after grafting organic amine to silica. The aminopropyl functional groups were successfully grafted on the MCF silica from ^{13}C and ^{29}Si MAS NMR results. The strong interaction between the NH_2 groups in the silane moieties and HPW molecules is shown by FT-IR, XPS and ^{31}P MAS-NMR. The HPW-NH_2-MCF is highly efficient in the *O*-heterocyclization of COD to 2,6-dihydroxy-9-oxabicyclo[3.3.1]nonane (**1**) and 2-hydroxy-9-oxabicyclo[3.3.1]nonane-6-one (**2**) with a COD conversion up to 100% and (**1** + **2**) selectivity up to 98%. The HPW-NH_2-MCF could be used for more than six times without any significant loss of activity and leaching of tungsten species in the reaction mixture. The good stability can be attributed to the strong interaction between the NH_2 groups in the silane moieties and HPW molecules.

Acknowledgements

We thank the Major State Basic Resource Development Program (Grant No. 2003CB 615807), NNSFC (Project 20973042), the Research Fund for the Doctoral Program of Higher Education (20090071110011) and the Science & Technology Commission of Shanghai Municipality (08DZ2270500) for financial support.

Notes and references

1 H. M. R. Hoffmann and J. Rabe, *Angew. Chem.*, 1985, **97**, 96.
2 S. M. Kupchan, M. A. Eakin and A. M. Thomas, *J. Med. Chem.*, 1971, **14**, 1147.
3 K. H. Lee and H. Furukawa, *J. Med. Chem.*, 1972, **15**, 609.
4 M. J. Rieser, J. F. Kozlowski, K. V. Wood and J. L. McLaughlin, *Tetrahedron Lett.*, 1991, **32**, 1137.
5 S. Behr, K. Hegemann, H. Schimanski, R. Frohlich and G. Haufe, *Eur. J. Org. Chem.*, 2004, **18**, 3884.
6 K. Hegemann, R. Frohlich and G. Haufe, *Eur. J. Org. Chem.*, 2004, **10**, 2181.
7 R. Gao, W. Dai, Y. Le, X. Yang, Y. Cao, H. Li and K. Fan, *Green Chem.*, 2007, **9**, 878.
8 R Gao, W. Dai, X. Yang, H. Li and K. Fan, *Appl. Catal., A*, 2007, **332**, 138.
9 M. T. Pope, *Heteropoly and Isopoly Oxometalates*, Springer-Verlag, New York, 1983.
10 J. F. Keggin, *Nature*, 1933, **131**, 908.
11 I. V. Kozhevnikov, *Catal. Rev.*, 1995, **37**, 311.
12 C. L. Hill and C. M. Prosser-McCartha, *Coord. Chem. Rev.*, 1995, **143**, 407.
13 T. Okuhara, N. Mizuno and M. Misono, *Adv. Catal.*, 1996, **41**, 113.
14 I. K. Song, S. H. Moon and W. Y. Lee, *Korean J. Chem. Eng.*, 1991, **8**, 33.
15 I. K. Song and M. A. Barteau, *Korean J. Chem. Eng.*, 2002, **19**, 567.
16 I. K. Song, M. S. Kaba and M. A. Barteau, *Langmuir*, 2002, **18**, 2358.
17 W. Chu, X. Yang, Y. Shan, X. Ye and Y. Wu, *Catal. Lett.*, 1996, **42**, 201.
18 N. Y. He, C. S. Woo, H. G. Kim and H. I. Lee, *Appl. Catal., A*, 2005, **281**, 167.
19 K. Nowinska, R. Formaniak and W. A. Waclaw, *Appl. Catal., A*, 2003, **256**, 115.
20 P. Kim, H. Kim, J. Yi and I. K. Song, *Stud. Surf. Sci. Catal.*, 2006, **159**, 265.
21 K. Nomiya, H. Murasaki and M. Miwa, *Polyhedron*, 1986, **5**, 1031.
22 M. Hasik, W. Turek, E. Stochmal, M. Łapkowski and A. Pron, *J. Catal.*, 1994, **147**, 544.
23 H. Kim, J. C. Jung, S. H. Yeom, K. Y. Lee and I. K. Song, *J. Mol. Catal. A: Chem.*, 2006, **248**, 21.
24 H. Kim, P. Kim, K. Y. Lee, S. H. Yeom, J. Yi and I. K. Song, *Catal. Today*, 2006, **111**, 361.
25 P. Schmidt-Winkel, W. W. Lukens, Jr., P. Yang, D. I. Margolese, J. S. Lettow, J. Y. Ying and G. D. Stucky, *Chem. Mater.*, 2000, **12**, 686.
26 D. Y. Zhao, J. L. Feng, Q. S. Huo, N. Melosh, G. H. Fredrickson, B. F. Chmelka and G. D. Stucky, *Science*, 1998, **279**, 548.
27 D. Y. Zhao, Q. S. Huo, J. L. Feng, B. F. Chmelka and G. D. Stucky, *J. Am. Chem. Soc.*, 1998, **120**, 6024.
28 J. S. Beck, J. C. Vartuli, W. J. Roth, M. E. Leonowicz, C. T. Kresge, K. D. Schmitt, C. T. W. Chu, D. H. Olson, E. W. Sheppard, S. B. McCullen, J. B. Higgins and J. L. Schlenker, *J. Am. Chem. Soc.*, 1992, **114**, 10834.
29 P. Schmidt-Winkel, W. W. Lukens Jr., D. Zhao, P. Yang, B. F. Chmelka and G. D. Stucky, *J. Am. Chem. Soc.*, 1999, **121**, 254.
30 A. S. M. Chong and X. S. Zhao, *J. Phys. Chem. B*, 2003, **107**, 12650.
31 F. Juan and E. Ruiz-Hitzky, *Adv. Mater.*, 2000, **12**, 430; A. M. Liu, K. Hidajat, S. Kawi and D. Y. Zhao, *Chem. Commun.*, 2000, 1145.
32 H. H. P. Yiu, P. A. Wright and N. P. Botting, *J. Mol. Catal. B: Enzym.*, 2001, **15**, 81.
33 N. Liu, R. A. Assink, B. Smarsly and C. J. Brinker, *Chem. Commun.*, 2003, 1146.
34 X. Wang, K. S. K. Lin, J. C. C. Chan and S. Cheng, *J. Phys. Chem. B*, 2005, **109**, 1763.
35 C. J. Dillon, J. H. Holles, R. J. Davis, J. A. Labinger and M. E. Davis, *J. Catal.*, 2003, **218**, 54.
36 S. Uchida, K. Inumaru and M. Misono, *J. Phys. Chem. B*, 2000, **104**, 8108.
37 S. Damyanova, J. L. G. Fierro, I. Sobrados and J. Sanz, *Langmuir*, 1999, **15**, 469.
38 H. L. Li, N. Perkas, Q. L. Li, Y. Gofer, Y. Koltypin and A. Gedanken, *Langmuir*, 2003, **19**, 10409.